

# **Author response on “Comparing turbulent parameters obtained from LITOS and radiosonde measurements” by A. Schneider et al.**

## **Anonymous Referee #1**

We thank the referee for his helpful comments. Below we cite each comment (indicated by italics) followed by our answer.

We would like to point out that our main focus is comparing dissipation rates from the Thorpe analysis as recently used by several authors with our own independent method. It is not primarily comparing  $L_O$  and  $L_T$ .

### **General comments**

*1) Is the comparison between  $L_T$  and  $L_O$  relevant in the way it is performed? To my opinion it is not. In the troposphere, the vertical extent of turbulent eddies frequently reach several hundred meters (as the Thorpe analysis confirms). The Thorpe length  $L_T$  is a second order statistic estimated within regions which vertical extent is significantly larger than  $L_T$  (two to three times). Now, you estimate  $L_O$  (Ozmidov length) with a vertical resolution of 10 m within a sliding window of 25 m. It is well known that turbulence is not homogeneous (it is indeed very intermittent as your measurements nicely illustrate). Is it meaningful to compare a second order statistics ( $L_T$ ) to local estimates of  $L_O$  (i. e. of epsilon) within constant height interval of 25 m. I suggest the authors to systematically perform some averaging on epsilon within the spatial domain where  $L_T$  is estimated before comparing  $L_T$  and  $L_O$ .*

Such an averaging is exactly what we have done. We have averaged both  $\epsilon$  and  $N$  over the unstable layers detected by the Thorpe method (in the following denoted by averaging brackets  $\langle \cdot \rangle$ ) and then computed the Ozmidov scale via  $\overline{L_O} = \sqrt{\langle \epsilon \rangle / \langle N \rangle^3}$ . The blue barplots in Fig. 3 and Fig. 7 show  $\overline{L_O}$  and  $\langle \epsilon \rangle$ , respectively, computed in that way. The cyan curves present the unaveraged quantities  $L_O = \sqrt{\epsilon / N^3}$  and  $\epsilon$  directly as measured by LITOS. We have made the description of our procedure clearer in the revised version.

p. 19040 l. 4 has been changed to: The energy dissipation rate (obtained from LITOS) is averaged over the layer (as detected by the Thorpe analysis of radiosonde data). Such means over a Thorpe layer will be denoted by averaging brackets  $\langle \cdot \rangle$ . For each unstable layer, the resulting  $\langle \epsilon \rangle$  is plugged into Eq. (2) to infer an Ozmidov scale  $\overline{L_O} = \sqrt{\langle \epsilon \rangle / \langle N \rangle^3}$  for the layer.

*A comparison of measurements can hardly be based on the comparison of outer scales if a constant window 25 m depth is used. An other way to compare measurements follows: for each 25 m window, a TKE dissipation rate, epsilon, is estimated. From epsilon, a variance of the wind velocity can be inferred by assuming a Kolmogorov spectrum. How this velocity variance compare to the turbulent potential energy (TPE) (which can be defined within the same window from the variance of the temperature fluctuations?).*

The size of the window at the computation of  $\varepsilon$  from the wind fluctuations measured by LITOS can be reduced, e. g., to 2 m with 1 m overlap. Then the  $\varepsilon$  profile shows more intermittency, as expected. Nevertheless, if the analysis of our paper is carried out with such a higher resolved  $\varepsilon$  profile, the results are similar, due to the averaging method mentioned above.

A comparison of TKE and TPE would indeed be interesting, as only few observational datasets are available and the fundamental understanding of turbulence may be improved. However, it is outside the scope of this paper.

*2) Second issue: is there cloudy air in the troposphere? If it is the case, the dry potential temperature profile used for the Thorpe sorting is not relevant. The effect of water vapor saturation must be considered by using a “moist” potential temperature profile (i. e. Wilson et al., 2013)*

We thank the referee for this suggestion. Originally we focussed on the stratosphere so that we did not consider moisture. In the revised version, we implement the method from Wilson et al. (2013) using the moist potential temperature. However, the difference between moist and dry computation is small. For BEXUS 12, the number of significant unstable layers changes from 259 to 254, the mean layer thickness from 50 m to 53 m, the mean Thorpe length in the troposphere from 26 m to 29 m. The mean dissipation rate has not changed significantly. For BEXUS 8, we originally used only the data from 7 km upwards. Now we have included the tropospheric data as well. Again, the difference between dry and moist computation is small; there is only one saturated layer, and only one significant unstable layer intersects with it, so that the averages do not change significantly.

At p. 19038 l. 16 we have inserted: Moisture is cared for using the routine given by Wilson et al. (2013). To this end, saturated regions are detected, and a composite potential temperature profile  $\Theta_*$  is computed by integration of  $\partial\Theta/\partial z$  using the moist buoyancy frequency within those saturated regions and the dry buoyancy frequency otherwise.

*3) I have some doubts (other than question 2) about the Thorpe analysis performed in this paper, especially in the troposphere. What is the mean trend-to-noise ratio (TNR) in the troposphere? What is the minimum size of the layers selected as turbulent? (the minimum  $L_T$  being 10 m, it suggests that you retain the inversion of two consecutive bins in the potential temperature profile as significant. Such a two bins layer is very dubious). If the mean TNR is smaller than unity, a pre-processing of the data is likely required. For instance, Wilson et al. (2011) decimated and filtered the potential temperature profile. Consequently, according to these authors, the minimum size of turbulent layers was  $\sim 50$  m in the troposphere.*

The Thorpe analysis shown in the discussion paper is carried out as described in Wilson et al. (2011) (assuming a dry atmosphere). The mean trend-to-noise ratio (TNR) is  $\bar{\xi} = 2.3$  for the BEXUS 8 flight and  $\bar{\xi} = 4.2$  for the BEXUS 12 flight; in the troposphere, we have  $\bar{\xi}_{\text{Tropo}} = 7.2$  for BEXUS 8 and  $\bar{\xi}_{\text{Tropo}} = 12$  for BEXUS 12. For the moist computation,  $\bar{\xi} = 1.7$  (BEXUS 8) and  $\bar{\xi} = 4.1$  (BEXUS 12). Nevertheless, we have several significant unstable layers with a thickness of 10 m or 20 m. Indeed, it is questionable whether such thin layers can unambiguously be reproduced by a radiosonde with 10 m resolution. But LITOS also shows thin layers of 10 m ... 20 m thickness. Ignoring the thin layers in radiosonde data, e. g., by smoothing of the  $\Theta$  profile prior to Thorpe sorting, would result in much less coincident layers especially in the stratosphere and, by this, would bias the comparison between both methods. In order to avoid any a-priori biases we take the thin layers in the radiosonde data into account, especially since they fulfil the criteria given by Wilson et al. (2011, 2010).

We have added at the end of Sect. 2 (p. 19039 l. 2): The mean trend-to-noise ratio (TNR) is  $\bar{\xi} = 1.7$  for the BEXUS 8 flight and  $\bar{\xi} = 4.1$  for the BEXUS 12 flight.

Several thin layers of only 10 m or 20 m passed the significance test. We are aware that this is on the edge of radiosonde capability. Nevertheless, LITOS also shows many thin layers. Ignoring the thin layers, e. g., by smoothing the  $\Theta_*$  profile prior to Thorpe sorting would result in much less coincident layers especially in the stratosphere and, by this, bias the comparison. In order to avoid any a-priori biases we take the significant thin layers in the radiosonde data into account.

## Specific comments

p. 19035, l. 3–4: *the statement about “static instability which drive turbulence” is unclear. The detected decreasing in potential temperature does not imply that static instability is the driving process. Turbulence driven by mechanical (shear) instability will also produce overturns (i. e. decreasing) in the potential temperature profile.*

p. 19043, l. 9: *Again, I do [not? author’s note] agree with the assertion that the instable layers detected by the Thorpe method are driven by convective instabilities*

Indeed, strong three-dimensional wind shear can also produce a potential temperature inversion. Such a negative  $\Theta$  gradient is by definition a static instability. But in this case you would not call the static instability the driver. We have changed our phrasing as follows:

p. 19035, l. 3–4: The evaluation uses the method developed by Thorpe (1977, 2005) to detect static instabilities as a proxy for turbulence.

p. 19043, l. 9: Not all turbulence is related to static instabilities. Even if initially a negative potential temperature gradient may have occurred, it is removed by the turbulent motions which outlive the instability;

p. 19036, l. 4: *A recent paper (Wilson et al., JASTP, 2014) shows few case studies of turbulent layers in the troposphere detected simultaneously by radar and balloon. Estimates of  $L_T$  and  $L_O$  are reported.*

We thank the referee for pointing out this paper which had eluded our notice. We take it into account in the revised version and have rephrased this sentence as follows:

But for the atmosphere there are only few examinations of the proportionality (e. g. Gavrilov et al., 2005; Kantha and Hocking, 2011; Wilson et al., 2014).

p. 19038, l. 11: *Please, explain this interval for epsilon (it does not correspond to the interval for  $l_0$ , i. e. fit error)*

The errors for  $l_0 = c\sqrt[4]{v^3/\varepsilon}$  and  $\varepsilon$  are related by Gaussian error propagation,

$$\Delta l_0 = \sqrt{\left(\frac{\partial l_0}{\partial \varepsilon}\right)^2 \Delta \varepsilon^2 + \left(\frac{\partial l_0}{\partial v}\right)^2 \Delta v^2} \approx \frac{c}{4} \frac{v^{3/4}}{\varepsilon^{5/4}} \Delta \varepsilon = \frac{l_0}{4\varepsilon} \Delta \varepsilon,$$

where the approximation neglects the error in the kinematic viscosity  $\nu$ , i. e.  $\Delta \nu = 0$ .

p. 19038, l. 11: *Is there an objective criterion in order to discriminate turbulent and non-turbulent spectra? Is it based on a visual check of each spectrum?*

The decision whether a spectrum is regarded as turbulent is made automatically based on objective criteria. First, the noise level is detected to select the fit range. If the noise level detection fails, the spectrum is sorted out. The fit of the Heisenberg spectrum is performed and then a set of criteria is applied to sort out bad fits, which occur for non-turbulent spectra. Those criteria are:

- The inner scale  $l_0$  has to be within the fit range.
- The value of  $\varepsilon$  has to be greater than zero and less than 100 (plausible values).
- The mean distance between the data and the fit has to be less than a given threshold.

p. 19038 l. 11 has been changed to: A spectrum is regarded as non-turbulent if the noise-level detection fails, if the inner scale  $l_0$  is not within the fit range, if  $\varepsilon$  has implausible values (less than zero or greater than 100 W/kg), or if the mean distance between the fit and the data is larger than a fixed threshold. That means the decision is made automatically based on a set of objective criteria.

p. 19039, l. 7: *The relatively low value for the mean  $L_T$  in the troposphere (26 m) is very likely due to the large number of occurrence of the small size inversions (10 or 15 m). According to me, such inversions cannot be detected from radiosondes: a statistics on the range of two or three points is not significant, especially if TNR is small.*

As described above (comment 3), we performed a significance test as suggested by Wilson et al. (2010). We agree that such thin layers are at the edge of the capability of the radiosonde analysis. Nevertheless we take these data into account to avoid a bias compared to our LITOS data showing similar thin layers.

p. 19039, l. 21: *The observation of turbulence at 21.73 km is done for a single height interval ( $\sim 25$  m). Turbulent layers of such a scale can hardly be detected by the Thorpe method from radiosondes (see Wilson et al. 2011 for instance). The lack of coincidence for such depths is not surprising.*

The referee is right that such thin layers are at the limit of radiosonde capabilities. Mainly we want to point out that there are turbulent layers not visible for the radiosondes (Thorpe method). For the revised version we select another altitude region which shows a larger turbulent layer ( $\sim 80$  m thickness) detected by LITOS but not by the Thorpe method.

p. 19040, l. 3–4: *What is the percentage of turbulent layers detected by both methods? And what is the scale of this simultaneous detection? (in other words, is the simultaneous detection dependent on the size of the turbulent layers?)*

We have added the following paragraph in the discussion after p. 19043 l. 15: Not all layers are detected by both systems. Of the significant layers detected by the Thorpe analysis, 86 % (BEXUS 8) and 69 % (BEXUS 12) are also detected by LITOS. For BEXUS 12, the mean thickness of significant unstable layers as detected by the Thorpe analysis is 53 m. The mean thickness of those significant layers also detected by LITOS is 63 m, that of significant layers not detected by LITOS only 31 m. That means that the simultaneous detection depends on the size of the layer; mainly thin layers are detected by only one method. But as this only applies to 30 % of the layers, and those layers were taken out of the comparison, the bias for our results should be small.

p. 19040, l. 15: *There is no scale for  $N$  (cyan curve) on the right panel of Fig. 3. The cyan curve ( $N$  ?) on the right panel of Fig. 3 is discontinuous. Why?*

Both blue and cyan curves show  $L_O$ ; the difference is that the cyan one has the full resolution of the  $\varepsilon$  profile from LITOS, while the blue barplot shows the mean over the unstable layers detected by the Thorpe method,  $\overline{L_O}$ , cf. (1) under general comments. We make this clearer in the revised version. The discontinuities originate from  $L_O = 0$  which cannot be shown in a logarithmic plot. There is no plot of  $N$  in that figure.

p. 19041, l. 5: *I suggest the authors to show the distributions of  $L_T$  and  $L_O$ ? Are they similar?*

We have extended Fig. 5 to show the distributions of the composite dataset of BEXUS 8 and BEXUS 12 (i.e. all data points seen in the graph) on the right and top axis, respectively. The histograms show a generally similar behaviour at scales larger than 10 m. The maximum for the Thorpe length is slightly larger than for the Ozmidov scale. At small scales  $L_T$  is limited by the resolution of the radiosonde which produces the cut-off at 10 m, while the histogram for  $\overline{L_O}$  shows a continuous decrease.

p. 19042, l. 5: *I agree with the way the comparison is performed. You could complete this plot with a scatter plot. Is there any correlation between the two estimates?*

There is no obvious relation between  $\varepsilon_{\text{LITOS}}$  and  $\varepsilon_{\text{Thorpe}}$ . The correlation coefficient between both is 0.39 for BEXUS 8 and 0.06 for BEXUS 12 (including moisture effects). The numbers will be mentioned in the revised version. We would like to avoid a scatter plot because it contains no additional information compared to Fig. 5 and Fig. 8.

p. 19042, l. 12: *Your study is not limited to stratospheric conditions.*

We have no overview about tropospheric studies, but want to point out that our study is at least the first for stratospheric conditions.

p. 19043, l. 6: *What is the size of the non-detected layers by the Thorpe method?*

The mean thickness of LITOS layers not intersecting a Thorpe layer for BEXUS 12 is 22 m. As expected this is quite close to the resolution of the radiosonde data.

p. 19043, l. 13: *What is the size of the detected layers by the Thorpe method which are not seen by LITOS? (I suspect that these layers are noise induced, they are likely of small vertical extent).*

The mean width of significant layers detected by the Thorpe method but not by LITOS is 31 m (BEXUS 12), i.e. they typically comprise several data points. As described above, we performed a significance test as suggested by Wilson et al. (2010). In the revised version, this information is in the paragraph mentioned above.

p. 19043, l. 21: *What is this limit?*

Window length and trend removal limit the frequency scales of the power spectral density on large scales (i.e. small frequencies). A reasonable part of the inertial range has to be resolved to enable a fit. Additionally, because the data points lie much less dense at large scales in the loglog plot, only few data points determine the fit at very large inner scales  $l_0$ . By visual inspection of real and artificial spectra with random  $l_0$ , the limit for a reliable fit is estimated to  $\sim 1$  m for a window length of 25 m. (The limit depends on the window length.) The largest  $l_0$  for the BEXUS 8 and BEXUS 12

flights is 10 cm and 8.7 cm, respectively. That is far away from the limit. In the revised version, the paragraph has been supplemented with this information.

We have changed our phrasing as follows: For large scales (i. e. low frequencies or small  $\varepsilon$ ), the detection limit is determined by the trend removal and the window length. As a reasonable part of the inertial range has to be resolved to enable a fit, the limit is estimated to  $\sim 1$  m. The maximal identified  $l_0$  values of 10 cm and 8.7 cm for BEXUS 8 and BEXUS 12, respectively, were far below this limit.

p. 19044, l. 1: *Your work certainly questions the Thorpe analysis (at least in the way you performed it, see remarks above), but also the LITOS results. Before comparing epsilon estimates, I suggest the authors to validate their TKE by comparing with TPE from temperature measurements.*

We do not question the Thorpe analysis as a whole. Fig 6 shows that mean  $\varepsilon$  are in reasonable agreement with our LITOS results (cf. p. 19044, l. 2–3). For individual layers we find large discrepancies in  $\varepsilon$ . We would like to point out that these discrepancies are expected, taking all the different published values for  $c^2$  into account. Also Wilson et al. (2014) report estimates of  $L_T$  and  $L_O$  for a limited number of layers which lead to values for  $c^2$  varying between 0.1 and 1.6. As mentioned above, the comparison of TKE and TPE is another fundamental topic that is outside the scope of this paper.

## **Anonymous Referee #2**

We thank the referee for the positive and stimulating feedback. As already mentioned in the manuscript, we agree that a 100 % correspondence in the detection of turbulent layers by both methods cannot be expected. The Thorpe analysis is only sensitive to layers with convective overturning (even if initially driven by wind shear), and LITOS is mainly sensitive to fully developed turbulence. Therefore we limited our analysis to layers visible by both methods and the lower vertical resolution of the Thorpe method.

Indeed, some quantitative relations between turbulent scales are still under debate. From this point of view the referee is right and our results are not surprising. Nevertheless, in the recent literature these relations are partly used to derive, e. g., energy dissipation rates, and uncertainties are partly neglected. Our method provides (for the first time) an independent test for these relations at spatial scales that cannot be resolved by, e. g., radars. We do not want to question the Thorpe method in general. Though, for individual layers further research on the temporal evolution of turbulence seems to be necessary. Therefore we fully agree with the reviewer that future research is essential. Accordingly we have added a note on this topic in the revised version of our manuscript.

# Comparing turbulent parameters obtained from LITOS and radiosonde measurements

A. Schneider, M. Gerding, and F.-J. Lübken

Leibniz-Institute of Atmospheric Physics at the University of Rostock, Kühlungsborn, Germany

Correspondence to: A. Schneider (schneider@iap-kborn.de)

**Abstract.** Stratospheric turbulence is important for the mixing of trace species and the energy balance, but direct measurements are sparse due to the required resolution and accuracy. Recently, turbulence parameters such as the energy dissipation rate  $\varepsilon$  were inferred from standard radiosonde data by means of a Thorpe analysis. To this end, layers with vertically decreasing potential temperature are analysed, which is expected to indicate turbulence. Such an application assumes a proportionality between the Thorpe length  $L_T$  and the Ozmidov scale  $L_O$ . While this relation is accepted for the ocean, experimental evidence for such proportionality in the stratosphere is sparse. We have developed a high-resolution (8 kHz) turbulence measurement system called LITOS, which for the first time resolves the inner scale of turbulence in the stratosphere. Therewith the energy dissipation rate  $\varepsilon$  can be determined by spectral analysis. This independent value for  $\varepsilon$  enables us to check the relation  $L_O \propto L_T$ . It turns out that no proportionality can be seen in our measurements. Furthermore, dissipation rates obtained from radiosondes deviate up to a factor of  $\sim 3000$  to those obtained by spectral analysis. Some turbulent layers measured by LITOS are not observed by the radiosonde at all, and vice versa.

## 1 Introduction

Although the stratosphere is mostly stably stratified, breaking of gravity waves and instabilities cause turbulence and energy dissipation. This modifies the energy transport from the troposphere to the mesosphere. The amount of energy converted into heat is described by the turbulent energy dissipation rate  $\varepsilon$ . Moreover, turbulence is an important parameter for the vertical mixing of trace species. As in the stratosphere turbulent dissipation occurs on small scales of centimetres and below, measurements are technically challeng-

ing and therefore sparse (e. g., Barat, 1982; Theuerkauf et al., 2011).

In order to enlarge the amount of turbulence measurements without complicated technical development, it has been proposed to extract turbulence parameters such as  $\varepsilon$  from standard radiosonde data (vertical resolution 5 m), as radiosoundings are performed daily from a worldwide net of stations (Clayson and Kantha, 2008). The evaluation uses the method developed by Thorpe (1977, 2005) to detect static instabilities as a proxy for turbulence. Note that such a measurement of a driving force is somewhat different from measuring the turbulent motions directly, as done by LITOS. For example, within an instability turbulence may have not yet been developed, or on the other hand, turbulence might be still active while the instability has already deceased. Additionally, turbulence may not be related to static instabilities at all.

The Thorpe analysis of unstable layers is done by comparing a measured potential temperature profile to an equivalent (statically) stable one obtained by sorting. This means that the order of the data points is changed upwards and downwards to yield a statically stable profile with monotonously increasing potential temperature. Precisely, the Thorpe displacement  $D_T$  is defined by the vertical displacements needed for the sorting, i. e. if an air parcel at altitude  $z_j$  is sorted to  $z_k$ , then the Thorpe displacement at  $z_j$  is  $D_T(z_j) = z_j - z_k$ . The Thorpe length is the root mean square of the Thorpe displacements taken over an unstable layer,

$$L_T := \text{rms}(D_T). \quad (1)$$

It describes the distance on which heavier air parcels are carried above lighter ones. Wilson et al. (2011, 2010) use the Thorpe method for statistical analysis without computing dissipation rates.

The Ozmidov length scale

$$L_O := \alpha \sqrt{\frac{\varepsilon}{N^3}}, \quad (2)$$

where  $\varepsilon$  is the (kinetic) energy dissipation rate,  $N$  the Brunt–Väisälä frequency and  $\alpha$  a numerical constant near unity, represents the vertical scales of the largest turbulent eddies (Ozmidov, 1965). For the determination of the dissipation rate from a Thorpe analysis, the key assumption is a proportionality between Thorpe and Ozmidov lengths,  $L_O \propto L_T$ . This relation has been extensively studied in the ocean, and the assumption is fulfilled to a good extent (Thorpe, 2005; Dillon, 1982; Wesson and Gregg, 1994). But for the atmosphere there are only few examinations of the proportionality (e.g. Gavrilov et al., 2005; Kantha and Hocking, 2011; Wilson et al., 2014). With our new high-resolved instrument LITOS (Leibniz-Institute Turbulence Observations in the Stratosphere) (Theuerkauf et al., 2011), the energy dissipation rate  $\varepsilon$  is obtained independent of  $L_T$  by means of spectral analysis of wind fluctuations. Thus it is possible to check the relation  $L_O \propto L_T$ .

Please note that our comparison involves two parameters: (a) evaluation method (Thorpe or spectral analysis) and (b) vertical resolution (low or high). We concentrate on results from high-resolved spectral analysis (as very precise method of  $\varepsilon$  determination) and low-resolved Thorpe analysis. Such a Thorpe evaluation of radiosonde data has been proposed for extensive use (Clayson and Kantha, 2008; Love and Geller, 2012). Note that Love and Geller (2012) call 1 Hz (5 m) high resolution, while we call it low resolution (compared to LITOS with 8 kHz). In principle, the Thorpe analysis can also be performed on data with higher resolution, as done, e.g., by Luce et al. (2002) for temperature data with 50 Hz sampling rate; however, these data are rarely available compared to standard radiosonde. Besides, a kind of spectral analysis can be used to determine dissipation rates from low-resolution wind data (Barat, 1982), but this method depends on the absolute value of the wind velocity which is not available for our measurements (see next section).

In Sect. 2, the measurement principle of LITOS and the determination of the energy dissipation rates with both methods are shortly reviewed. The independent measurements of  $L_O$  and  $L_T$  are compared in Sect. 3. Section 4 shows results for the energy dissipation rate  $\varepsilon$  from both a Thorpe analysis and our high-resolved spectral analysis. Conclusions are drawn in Sect. 5.

## 2 Instrumentation and methods

As described in Theuerkauf et al. (2011), LITOS is a balloon-borne instrument which measures winds with high vertical resolution of millimetres. The wind sensor is a constant temperature anemometer (CTA), which facilitates the cooling effect on a heated wire of 5  $\mu\text{m}$  diameter. To infer wind velocities from the anemometer voltage, a calibration in the same ambient conditions (pressure, temperature) is required. This is not possible for a balloon flight, as the pressure varies within several orders of magnitude during the flight. Nev-

ertheless, we are only interested in the spectral form, and the absolute values are not important (see below); therefore we use the anemometer voltage for the analysis. The vertical resolution is obtained by applying a sample rate of 8 kHz with a balloon ascent rate of 5  $\text{m s}^{-1}$ . Up to date, three flights on large ( $\sim 10000 \text{ m}^3$ ) balloons were performed, namely BEXUS 6, 8 and 12 in 2008, 2009 and 2011, respectively. They were launched at Kiruna (68° N, 21° E) in autumn. For BEXUS 6, the radiosonde data are partly disturbed so that it is not considered in this article.

The left panel in Fig. 1 shows an example of a time series of the anemometer voltage of the BEXUS 12 flight. Large-scale motions have already been removed by subtracting a spline. At altitudes with small variations ( $\lesssim 1 \text{ mV}$ , e.g., from 10.28 to 10.3 km), the signal mainly shows instrumental noise; this corresponds to a calm region. Large fluctuations, as in the height range of 10.18 to 10.28 km, correspond to turbulence. Note that there is a sub-structure which divides the turbulent region into different patches. For the patch from 10.27 to 10.28 km (shaded in the graph), the power spectral density (PSD) is plotted in the right panel of Fig. 1 (blue curve). An inertial regime with a  $-5/3$  slope and the transition to the viscous subrange with a  $-7$  slope is identified. The part below  $\sim 10^{-2} \text{ m}$  spatial scale with approximately constant PSD corresponds to the instrumental noise level. As the transition to the inertial range is resolved, a fit of the Heisenberg (1948) model in the form given by Lübken (1992) is applied to the experimental data (red curve). This gives the inner scale  $l_0$ , i.e. the transition from the inertial to the viscous subrange. In the example,  $l_0 = 1.9 \times 10^{-2} \text{ m} \pm 4.5 \times 10^{-3} \text{ m}$  (fit error). Note that  $l_0$  does not depend on the absolute value of the PSD, only on identifying the bend in the spectrum. From the inner scale, the energy dissipation rate is obtained by

$$\varepsilon = c^4 \frac{\nu^3}{l_0^4}, \quad (3)$$

where  $\nu$  is the kinematic viscosity (derived from the radiosonde measurement of temperature and pressure on the same gondola), and  $c = 5.7$  (Theuerkauf et al., 2011; Haack et al., 2014). For the example in Fig. 1,  $\varepsilon = 3.2 \times 10^{-4} \text{ W kg}^{-1} \pm 3.0 \times 10^{-4} \text{ W kg}^{-1}$ .

In order to obtain a vertical profile of energy dissipation rate, a sliding window of 5 s (roughly 25 m altitude) is used. For each window,  $\varepsilon$  is computed according to the procedure described above. For non-turbulent spectra,  $\varepsilon$  is set to zero. ~~See Haack et al. (2014) for details.~~ A spectrum is regarded as non-turbulent if the noise-level detection fails, if the inner scale  $l_0$  is not within the fit range, if  $\varepsilon$  has implausible values (less than zero or greater than 100  $\text{W/kg}$ ), or if the mean distance between the fit and the data is larger than a fixed threshold. That means the decision is made automatically based on a set of objective criteria. The resulting  $\varepsilon$  profile has a vertical resolution of  $\sim 10 \text{ m}$  due to the selected overlap.



The Thorpe analysis is performed according to the procedure described in Wilson et al. (2011) on data from a Vaisala RS92 radiosonde, which was on the same gondola as the CTA sensors. Moisture is cared for using the routine given by Wilson et al. (2013). To this end, saturated regions are detected, and a composite potential temperature profile  $\Theta_*$  is computed by integration of  $\partial\Theta/\partial z$  using the moist buoyancy frequency within those saturated regions and the dry buoyancy frequency otherwise. The left panel of Fig. 2 shows the potential temperature profile for the BEXUS 12 flight. In the inset, the part from 15.35 to 15.80 km is magnified for better visibility of instabilities, which manifest as negative gradients of potential temperature. The Thorpe displacement is shown in the right panel of Fig. 2. Large displacements correspond to large vertical extents of unstable layers. To identify unstable layers and their vertical extension, the cumulative sum of the Thorpe displacement (which is negative within an unstable region and zero within a stable one) is used. To select real overturns and discard negative potential temperature gradients originating from measurement noise, a statistical test is applied. To this end, the range of the potential temperatures within an inversion is compared with the range of a pure noise sample of the same length with standard deviation of the measurement noise (Wilson et al., 2010). For each detected unstable layer, the Thorpe length is computed according to Eq. (1). Only significant overturns with a 99 % percentile are used, discarding  $\sim 45\%$  (BEXUS 8) and  $\sim 30\%$  (BEXUS 12), respectively, of the inversions as noise-induced. The mean trend-to-noise ratio (TNR) is  $\xi = 1.7$  for the BEXUS 8 flight and  $\xi = 4.1$  for the BEXUS 12 flight.

Several thin layers of only 10 m or 20 m passed the significance test. We are aware that this is on the edge of radiosonde capability. Nevertheless, LITOS also shows many thin layers. Ignoring the thin layers, e. g., by smoothing the  $\Theta_*$  profile prior to Thorpe sorting would result in much less coincident layers especially in the stratosphere and, by this, bias the comparison. In order to avoid any a-priori biases we take the significant thin layers in the radiosonde data into account.

### 3 Comparison of Thorpe and Ozmidov scales

A plot of the Thorpe length for the BEXUS 12 flight is shown in the left panel of Fig. 3. Unstable layers take up 50 % of the altitude and can be found in the whole range. Large Thorpe lengths stand out, e. g., at 5 km, between 5 and 10 km and near 25 km altitude, corresponding to the large values of  $D_T$  in the right panel of Fig. 2. Mean values of  $L_T$  are 29 m in the troposphere and 22 m in the stratosphere, i. e. the Thorpe length is slightly larger in the less stable troposphere.

The Ozmidov scale is computed from the energy dissipation rate obtained by LITOS, using Eq. (2) and  $\alpha = 1$ . The Brunt–Väisälä frequency  $N$  is calculated from the radiosonde

data as it only slowly varies with altitude. In that computation, the sorted potential temperature profile is used instead of the original data, because a background stratification is needed and an imaginary  $N$  shall be avoided (Dillon, 1982, Sect. 3). The result for the BEXUS 12 flight is plotted in the right panel of Fig. 3 (cyan curve). According to LITOS, 53 % of the atmosphere is turbulent, i. e.  $\varepsilon > 0$  and hence  $L_O > 0$ .

Figure 4 shows the Thorpe length and the Ozmidov scale for the altitude range of 15.35 km to 15.80 km. As LITOS computes  $\varepsilon$  on a constant grid independent of the layers, the substructure of larger turbulent layers can be seen (e. g., from  $\sim 15.5$  km to 15.62 km), while the Thorpe length is a per-layer value by construction. Some layers are only detected by either LITOS or the radiosonde. For example, from 15.410 km to 15.443 km and from 15.706 km to 15.789 km LITOS observes turbulence while the Thorpe method does not. At the first mentioned altitude region, the potential temperature gradient is positive (see inset on the left panel of Fig. 2), so that the Thorpe method is blind for the turbulent motions. At the second one, the decrease of potential temperature is not significant. On the other hand, from 15.384 km to 15.401 km and from 15.455 km to 15.475 km, the Thorpe analysis observes instability while no turbulent motions can be detected by LITOS. Potentially, turbulence has not yet been developed by the static instability detected by the Thorpe method. A final answer cannot be given from our data. The slightly different altitudes of layers observed by both systems might be due to quantisation effects.

In order to do a comparison between both length scales, the layers where both methods detect turbulence are selected. For BEXUS 8 (BEXUS 12), 86 % (69 %) of the significant unstable layers are also detected by LITOS, and 90 % (88 %) of the layers detected by LITOS intersect with a significant unstable layer. The energy dissipation rate (obtained from LITOS) is averaged over the layer (as detected by the Thorpe analysis of radiosonde data). Such means over a Thorpe layer will be denoted by averaging brackets  $\langle \cdot \rangle$ . For each unstable layer, the resulting  $\langle \varepsilon \rangle$  is plugged into Eq. (2) to infer an Ozmidov scale  $\bar{L}_O = \sqrt{\langle \varepsilon \rangle / \langle N \rangle^3}$  for the layer. The blue curve in the right panel of Fig. 3 shows a plot for the BEXUS 12 flight. The layer near 5 km with large  $L_T$ , e. g., is also seen in  $\bar{L}_O$ , but less pronounced. In contrast, at  $\sim 10$  km altitude the Ozmidov scale is larger than the Thorpe scale. Mean values of  $\bar{L}_O$  are 15 m in the troposphere and 6 m (i. e. only half the value) in the stratosphere. Thus, in qualitative agreement with Eq. (2), the less stable troposphere shows on average a larger Ozmidov scale, i. e. larger eddies. As the Thorpe length shows a similar behaviour (see above), this generally supports the assumption of a relation between  $L_T$  and  $L_O$ .

In Fig. 5 Ozmidov scale  $\bar{L}_O$  and Thorpe length  $L_T$  are plotted against each other for those 136 (175) significant unstable layers of the BEXUS 8 (BEXUS 12) flight where turbulence has been detected by LITOS. Both length scales are in the same order of magnitude, but no direct relation between

them can be seen in either flight. The correlation coefficient between both is 0.32 for BEXUS 8 and 0.33 for BEXUS 12. Note that  $L_T$  is limited by the resolution of the radiosonde ( $\sim 10$  m).

The histograms at the top and right axes in Fig. 5 show the distributions for  $\overline{L_O}$  and  $L_T$ , respectively, for the composite dataset of BEXUS 8 and BEXUS 12. The maximum for the Thorpe length is slightly larger than for the Ozmidov scale. The decrease towards large scales is similar for both lengths. At small scales  $L_T$  is limited by the resolution of the radiosonde which produces the cut-off at 10 m, while the histogram for  $\overline{L_O}$  shows a continuous decrease.

In contrast to our measurements, an approximate proportionality between Thorpe and Ozmidov lengths is observed in the ocean (e. g., Dillon, 1982; Wesson and Gregg, 1994; Thorpe, 2005). For example, Wesson and Gregg (1994) find that most of their data fall between  $L_O = 4L_T$  and  $L_O = (1/4)L_T$  with a range from  $10^{-2}$  m to  $10^2$  m. This is the basis for applying the Thorpe analysis on atmospheric data. Several authors (e. g., Gavrilov et al., 2005; Clayson and Kantha, 2008; Kantha and Hocking, 2011) inferred energy dissipation rates from the Thorpe analysis by plugging  $L_O = cL_T$  into Eq. (2) and solving for  $\varepsilon$ , thus getting

$$\varepsilon = c^2 L_T^2 N^3. \quad (4)$$

Knowledge about the constant  $c^2$  is very limited (see discussion below), and only Gavrilov et al. (2005) provide some information based on stratospheric data. With our high-resolution wind data we can determine this constant independently. Wijesekera et al. (1993) found the distribution of the ratio  $L_T/L_O$  to be lognormal, which implies  $(L_O/L_T)^2 = c^2$  to be lognormal as well. Logarithmic histograms of  $(\overline{L_O}/L_T)^2$  for the BEXUS 8 and BEXUS 12 flights are presented in Fig. 6. The red curves display the most likely normal distributions for the logarithmic data. They show a sufficient agreement to the histograms and are both centred around  $\sim 0.1$  and  $\sim 0.1$ , respectively. The distribution of values is fairly broad: the full width half maximum (FWHM) spans  $\sim 1.9$  and  $\sim 1.9$  orders of magnitude, respectively.

#### 4 Energy dissipation rates

The relation between the energy dissipation rate  $\varepsilon$  and the length scales discussed above involves the Brunt–Väisälä frequency, see Eqs. (2) and (4). Thus the  $\varepsilon$  values computed from LITOS via spectral analysis and the ones from the radiosonde via Thorpe analysis have to be compared separately.

The left panel of Fig. 7 shows an altitude profile of energy dissipation rates obtained from the Thorpe analysis of the radiosonde on BEXUS 12, assuming  $L_O = cL_T$  with  $c^2 = 0.3$  as in Clayson and Kantha (2008). In the right panel, the altitude profile of energy dissipation obtained from LITOS is plotted in cyan, while the blue curve depicts the mean  $\langle \varepsilon \rangle$

over the unstable layers detected by the Thorpe analysis, for comparability. On average, the values are in the same order of magnitude, and the profiles have a similar structure. The large dissipation near  $\sim 10$  km in the CTA data does not stand out in the Thorpe analysis. The mean value over all significant unstable layers from Thorpe,  $1 \text{ mW kg}^{-1}$ , is larger than the one from LITOS,  $0.3 \text{ mW kg}^{-1}$ . For BEXUS 8 the averages are  $3 \text{ mW kg}^{-1}$  from Thorpe and  $2 \text{ mW kg}^{-1}$  from LITOS. That fits to the fact that the used value for  $c^2$ , 0.3, is larger than the one obtained from our own data,  $c^2 = 0.1$  (cf. Fig. 6). If the whole  $\varepsilon$  profile (not only the unstable layers detected by Thorpe) is taken into account, the average dissipation rate obtained by LITOS is  $0.4 \text{ mW kg}^{-1}$  for BEXUS 12 and  $2 \text{ mW kg}^{-1}$  for BEXUS 8. To get a closer look, the deviation of  $\langle \varepsilon \rangle$  from LITOS to  $\varepsilon$  inferred from the Thorpe analysis indicated by the ratio  $\langle \varepsilon_{\text{LITOS}} \rangle / \varepsilon_{\text{Thorpe}}$  of the blue and green curves in Fig. 7 is plotted in Fig. 8. It reveals a large range of 5 orders of magnitude. Overall, for 71 % (BEXUS 8: 64 %) of the layers,  $\varepsilon$  inferred from the Thorpe analysis is larger than the value from the spectral analysis. That the ratio is sometimes larger and sometimes smaller than unity illustrates that the most likely value of  $c^2$  does not contain the whole information, but the width of the distribution is important. The correlation coefficient between  $\langle \varepsilon_{\text{LITOS}} \rangle$  and  $\varepsilon_{\text{Thorpe}}$  is 0.06 (BEXUS 8: 0.39). Due to the influence of the Brunt–Väisälä frequency, pronounced peaks in  $L_O$  or  $L_T$  (Fig. 3) do not necessarily correspond to large  $\varepsilon$  (Fig. 7), e. g., at  $\sim 5$  km.

#### 5 Discussion and conclusions

In this paper, the first extensive examination of the relation between the Thorpe length  $L_T$  and Ozmidov scale  $L_O$  for stratospheric conditions was performed, using the new high-resolution instrument LITOS and a radiosonde on the same gondola. Therewith, the assumption for computing energy dissipation rates  $\varepsilon$  from a Thorpe analysis of standard radiosondes, namely the proportionality  $L_O \propto L_T$ , was checked. In our data no obvious relation between  $\overline{L_O}$  and  $L_T$  can be seen, particularly no proportionality. The proportionality “constant” used in radiosonde analyses,  $c^2 = (\overline{L_O}/L_T)^2$ , shows a very broad distribution with a width of  $\sim 2$  orders of magnitude. This is also reflected in the large deviation of  $\varepsilon$  values up to a factor of  $\sim 3000$  obtained with both methods. Nevertheless, although the values for individual layers are highly variable, the mean of  $c^2$  is 0.1 for both BEXUS 12 and 0.1 for BEXUS 8, respectively, which is close to 0.3 used by Clayson and Kantha (2008), who reviewed oceanic measurements to obtain that value. Kantha and Hocking (2011) obtained  $c^2 = 1.0$  by a comparison of radiosonde data to radar measurements. Gavrilov et al. (2005) used  $c^2 = 1.32$  ( $c = 1.15$ ) referring to a French thesis; this value was obtained from selected thick stratospheric layers ( $> 200$  m) with statistically homogeneous turbulence. However, in those publications no data basis, distribution width or

error is given. Recently, Wilson et al. (2014) reported a few case studies of turbulent layers in the troposphere detected simultaneously by radar and balloon; using their reported estimates of  $L_T$  and  $L_O$  leads to values of  $c^2$  between 0.1 and 1.6.

One reason for discrepancies from the proportionality  $L_O \propto L_T$  may be that large overturns might change significantly during the time the sensor needs to fly through the layer, so that the sorting procedure makes no sense anymore. Furthermore, direct numerical simulations by Smyth and Moum (2000) indicate that  $L_O/L_T$  is not constant, but depends on the age of turbulence.

Some turbulent layers are not detected at all by the Thorpe analysis. Those are not associated with a (significant) negative gradient of potential temperature, which is necessary for detection by the Thorpe method. Not all turbulence is related to static instabilities. Even if initially a negative potential temperature gradient may have occurred, it is removed by the turbulent motions which outlive the instability; such fossil turbulence cannot be detected by the Thorpe method. Apart from that, turbulent layers may be too thin to be observed with the relatively coarse vertical resolution of the radiosonde. On the other hand, some unstable layers detected by the Thorpe analysis are not observed by LITOS. An explanation is that the static instability may not yet have lead to turbulent motions. In these cases, a correspondence between both measurements is not expected.

Not all layers are detected by both systems. Of the significant layers detected by the Thorpe analysis, 86 % (BEXUS 8) and 69 % (BEXUS 12) are also detected by LITOS. For BEXUS 12, the mean thickness of significant unstable layers as detected by the Thorpe analysis is 53 m. The mean thickness of those significant layers also detected by LITOS is 63 m, that of significant layers not detected by LITOS only 31 m. That means that the simultaneous detection depends on the size of the layer; mainly thin layers are detected by only one method. But as this only applies to  $\lesssim 30\%$  of the layers, and those layers were taken out of the comparison, the bias for our results should be small.

For LITOS, the detection limit for  $l_0$  on small scales (i. e. high frequencies or large  $\epsilon$ ) is given by the sampling rate. This limit has been encountered in a few cases for small regions where the inertial range extends further than the Nyquist limit of 4 kHz. For large scales (i. e. low frequencies or small  $\epsilon$ ), the detection limit is determined by the trend removal and the window length. As a reasonable part of the inertial range has to be resolved to enable a fit, the limit is estimated to  $\sim 1$  m. The maximal identified  $l_0$  values of 10 cm and 8.7 cm for BEXUS 8 and BEXUS 12, respectively, were far below this limit. That means that these limitations do not affect the results.

Up to date, we have only two flights with data usable for the analysis presented in this paper, namely BEXUS 8 and BEXUS 12, which both took place at polar latitudes near autumn equinox. Of course they cannot represent the

whole variability of the stratosphere. Nevertheless, although there are differences between both flights, such as dissipation rates being on average one order of magnitude higher for BEXUS 8, these are not relevant for the results discussed above. More flights with our new high-resolution instrument are planned to broaden the data basis.

Our results question the applicability of the Thorpe analysis for the extraction of energy dissipation rates for individual turbulent layers. Nevertheless, statements in the statistical mean seem to be possible. Further research on the relation between Thorpe and Ozmidov lengths and the temporal evolution of turbulence is necessary.

*Acknowledgements.* The data from the BEXUS 8 flight were kindly provided by Anne Haack. The BEXUS programme was financed by the German Aerospace Center (DLR) and the Swedish National Space Board (SNSB). We are grateful for the support by the “International Leibniz Graduate School for Gravity Waves and Turbulence in the Atmosphere and Ocean” (ILWAO) funded by the Leibniz Association (WGL). Furthermore, we would like to thank Lars Umlauf for helpful discussions.

## References

- Barat, J.: Some characteristics of clear-air turbulence in the middle stratosphere, *J. Atmos. Sci.*, 39, 2553–2564, doi:10.1175/1520-0469(1982)039<2553:SCOCAT>2.0.CO;2, 1982.
- Clayson, C. A. and Kantha, L.: On turbulence and mixing in the free atmosphere inferred from high-resolution soundings, *J. Atmos. Ocean. Tech.*, 25, 833–852, doi:10.1175/2007JTECHA992.1, 2008.
- Dillon, T. M.: Vertical overturns: A comparison of Thorpe and Ozmidov length scales, *J. Geophys. Res.*, 87, 9601–9613, 1982.
- Gavrilov, N. M., Luce, H., Crochet, M., Dalaudier, F., and Fukao, S.: Turbulence parameter estimations from high-resolution balloon temperature measurements of the MUTSI-2000 campaign, *Ann. Geophys.*, 23, 2401–2413, doi:10.5194/angeo-23-2401-2005, 2005.
- Haack, A., Gerding, M., and Lübken, F.-J.: Characteristics of stratospheric turbulent layers measured by LITOS and their relation to the Richardson number, *J. Geophys. Res.*, 119, 10 605–10 618, doi:10.1002/2013JD021008, 2014.
- Heisenberg, W.: Zur statistischen Theorie der Turbulenz, *Z. Phys.*, 124, 628–657, doi:10.1007/BF01668899, 1948.
- Kantha, L. and Hocking, W.: Dissipation rates of turbulence kinetic energy in the free atmosphere: MST radar and radiosondes, *J. Atmos. Sol.-Terr. Phys.*, 73, 1043–1051, doi:10.1016/j.jastp.2010.11.024, 2011.
- Love, P. T. and Geller, M. A.: Research using high (and higher) resolution radiosonde data, *T. Am. Geophys. Un.*, 93, 337–338, doi:10.1029/2012EO350001, 2012.
- Lübken, F.-J.: On the extraction of turbulent parameters from atmospheric density fluctuations, *J. Geophys. Res.*, 97, 20 385–20 395, doi:10.1029/92JD01916, 1992.
- Luce, H., Fukao, S., Dalaudier, F., and Crochet, M.: Strong Mixing Events Observed near the Tropopause

- with the MU Radar and High-Resolution Balloon Techniques, *J. Atmos. Sci.*, 59, 2885–2896, doi:10.1175/1520-0469(2002)059<2885:SMEONT>2.0.CO;2, 2002.
- Ozmidov, R. V.: On the turbulent exchange in a stably stratified ocean, *Izv. AN. Fiz. Atmos. Ok.*, 1, 853–860, translated from Russian by Danielle and Victor Barcion, 1965.
- Smyth, W. D. and Moum, J. N.: Length scales of turbulence in stably stratified mixing layers, *Phys. Fluids*, 12, 1327–1342, doi:10.1063/1.870385, 2000.
- Theuerkauf, A., Gerding, M., and Lübken, F.-J.: LITOS – a new balloon-borne instrument for fine-scale turbulence soundings in the stratosphere, *Atmos. Meas. Tech.*, 4, 55–66, doi:10.5194/amt-4-55-2011, 2011.
- Thorpe, S. A.: Turbulence and mixing in a Scottish loch, *Philos. Tr. R. Soc. S-A*, 286, 125–181, doi:10.1098/rsta.1977.0112, 1977.
- Thorpe, S. A.: *The Turbulent Ocean*, Cambridge University Press, Cambridge, section 6.3.2, 2005.
- Wesson, J. C. and Gregg, M. C.: Mixing at Camarinal Sill in the Strait of Gibraltar, *J. Geophys. Res.*, 99, 9847–9878, doi:10.1029/94JC00256, 1994.
- Wijesekera, H. W., Dillon, T. M., and Padman, L.: Some statistical and dynamical properties of turbulence in the oceanic pycnocline, *J. Geophys. Res.*, 98, 22 665–22 679, doi:10.1029/93JC02352, 1993.
- Wilson, R., Luce, H., Dalaudier, F., and Lefrère, J.: Turbulence patch identification in potential density or temperature profiles, *J. Atmos. Ocean. Tech.*, 27, 977–993, doi:10.1175/2010JTECHA1357.1, 2010.
- Wilson, R., Dalaudier, F., and Luce, H.: Can one detect small-scale turbulence from standard meteorological radiosondes?, *Atmos. Meas. Tech.*, 4, 795–804, doi:10.5194/amt-4-795-2011, 2011.
- Wilson, R., Luce, H., Hashiguchi, H., Shiotani, M., and Dalaudier, F.: On the effect of moisture on the detection of tropospheric turbulence from in situ measurements, *Atmos. Meas. Tech.*, 6, 697–702, doi:10.5194/amt-6-697-2013, 2013.
- Wilson, R., Luce, H., Hashiguchi, H., Nishi, N., and Yabuki, Y.: Energetics of persistent turbulent layers underneath mid-level clouds estimated from concurrent radar and radiosonde data, *J. Atmos. Sol.-Terr. Phys.*, 118, Part A, 78–89, doi:10.1016/j.jastp.2014.01.005, 2014.

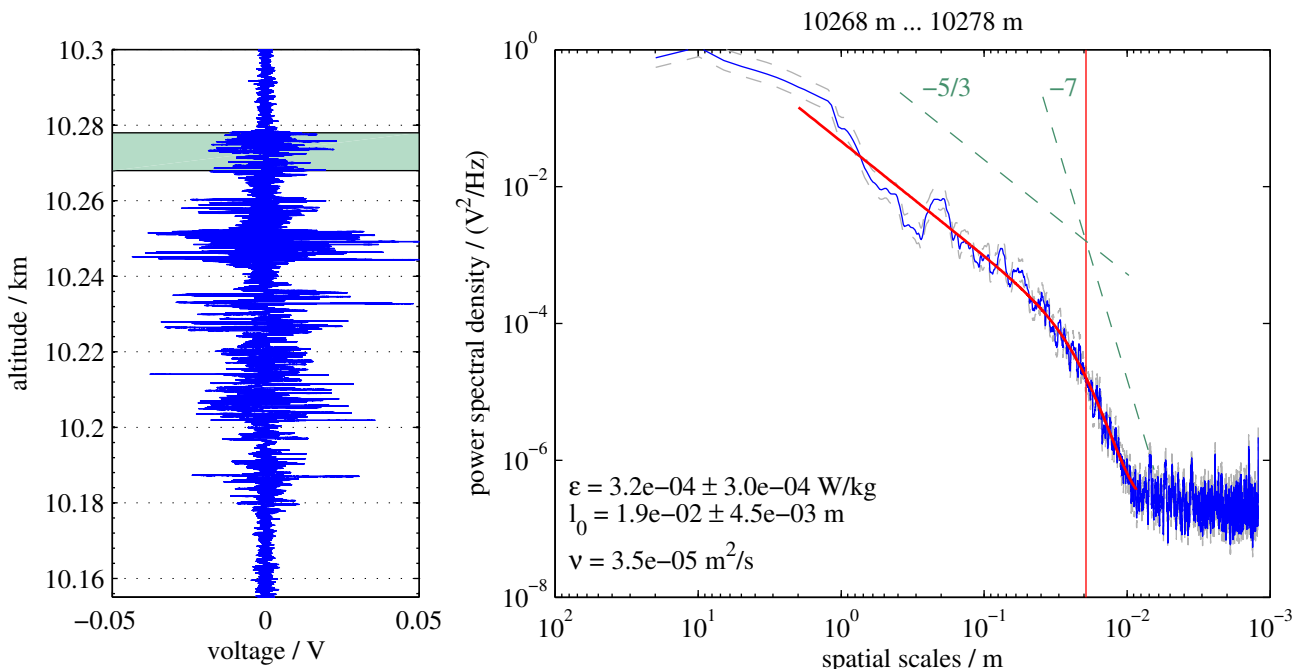


**Figure 1.** Example of raw data (left) and associated power spectrum (right) computed for the shaded area in the raw data plot. In the raw data, an amplitude of  $\lesssim 1$  mV corresponds to instrumental noise. In the spectrum, the blue curve shows the measurement, the grey dashed lines the 95 % confidence interval and the red curve the fit of the Heisenberg model to the measured spectrum, the red vertical line indicates the inner scale  $l_0$ . The green dashed lines visualise slopes of  $-5/3$  and  $-7$ . The errors given are fit errors.

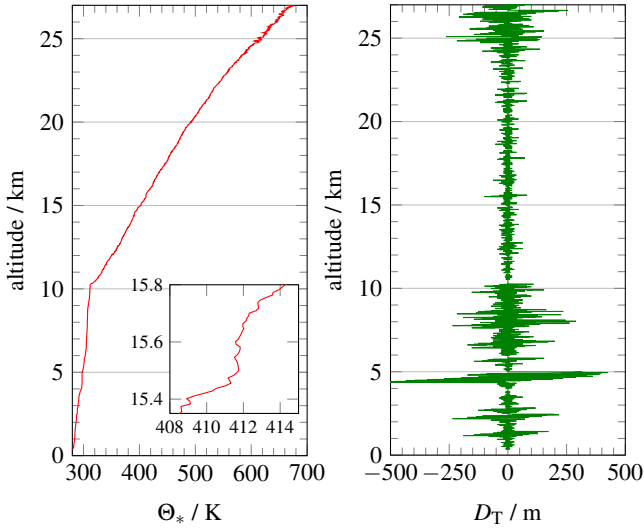


**Figure 2.** Potential temperature profile (left) and Thorpe displacement (right) for the BEXUS 12 flight. The inset in the left panel shows a magnification from 15.35 to 15.80 km for better visibility of instabilities (manifested as negative gradients of potential temperature).

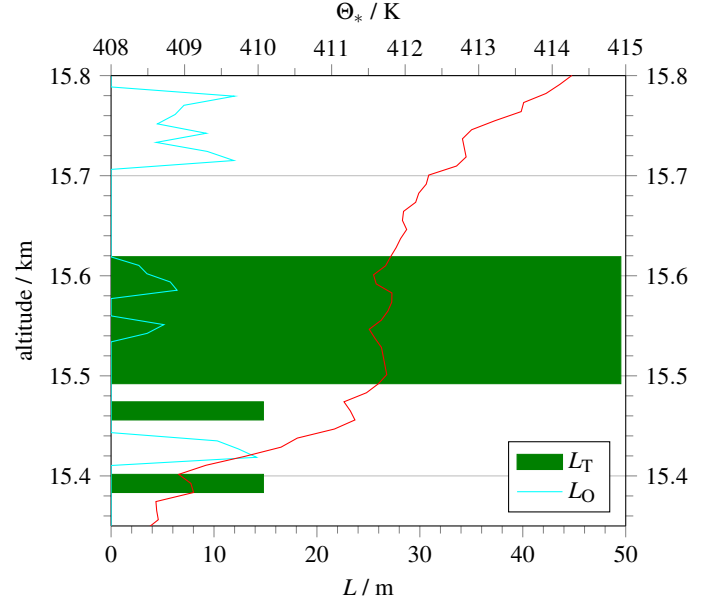


**Figure 4.** Detail plot of Thorpe (green) and Ozmidov (cyan) scales for the BEXUS 12 flight. The potential temperature is plotted in red.

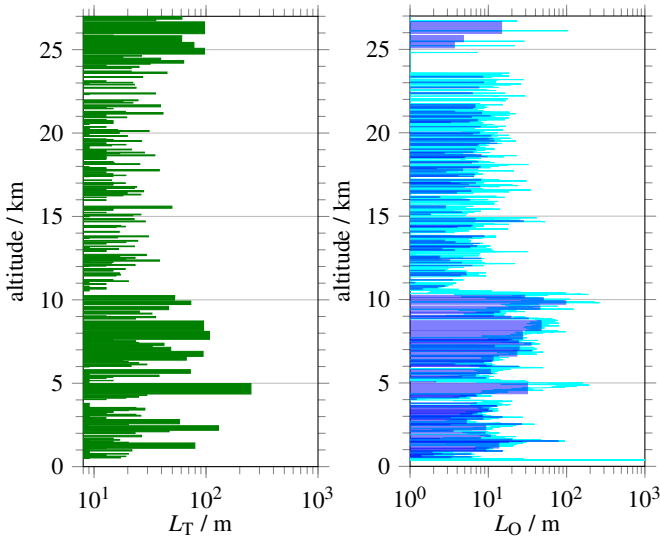


**Figure 3.** Thorpe length (left) and Ozmidov scale (right) vs. altitude for the detected inversions of the BEXUS 12 flight. The cyan curve shows the Ozmidov scale  $L_O$  in the full resolution of the LITOS profile, the blue one averages over the inversions detected by the radiosonde ( $\bar{L}_O$ ).

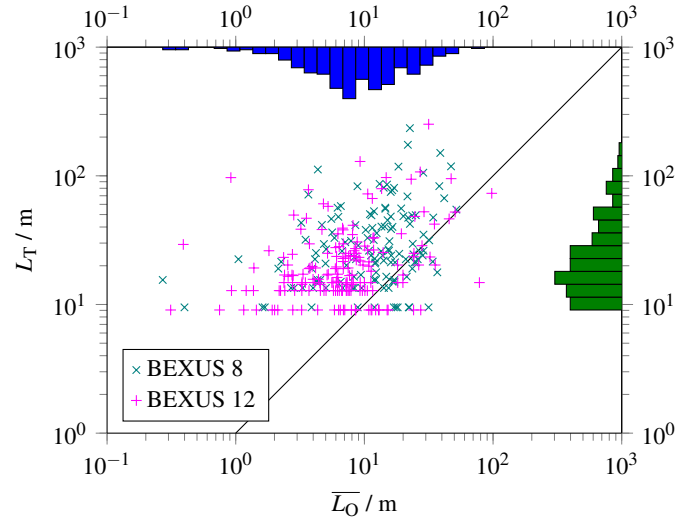


**Figure 5.** Thorpe scale  $L_T$  vs. Ozmidov scale  $\bar{L}_O$  for the BEXUS 8 (green) and 12 (magenta) flights. The black diagonal line represents  $L_O = L_T$ . The histograms show the distributions of  $L_O$  and  $L_T$ , respectively, of the composite data set of BEXUS 8 and BEXUS 12, i. e. of all data points in the graph. The occurrence axes have a linear scale and are omitted due to readability. Note that  $L_T$  is limited by the resolution of the radiosonde ( $\sim 10$  m).

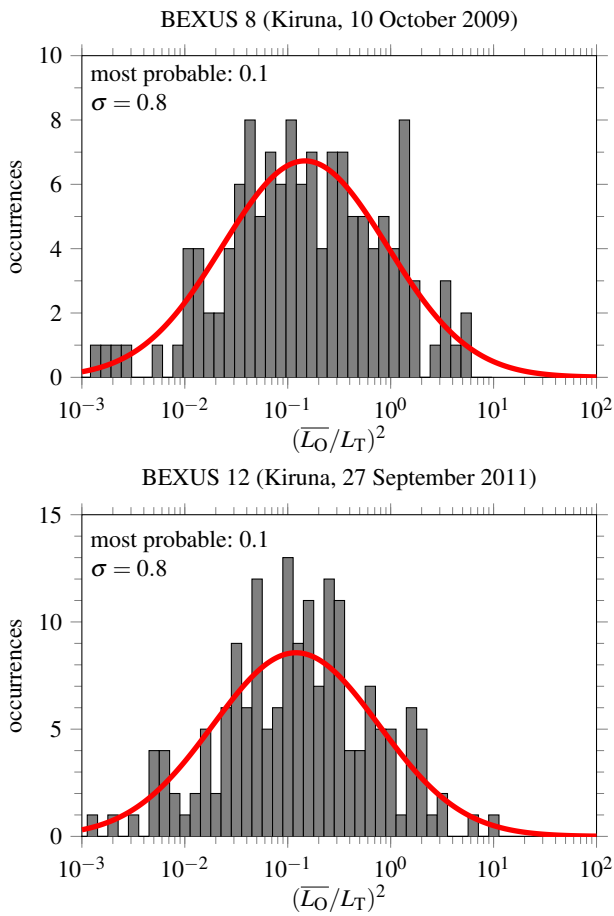


**Figure 6.** Statistics for the ratio  $(\overline{L_O}/L_T)^2$  for the BEXUS 8 (top) and BEXUS 12 (bottom) flights. The red curves show the most likely normal distributions for the logarithmic data.

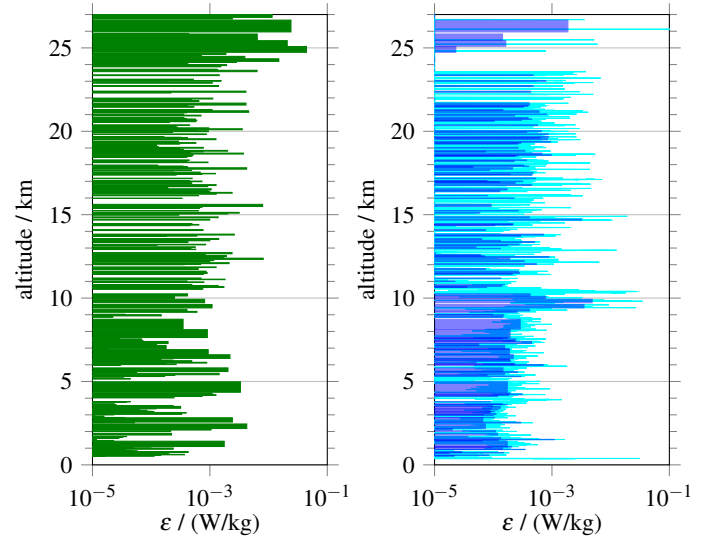


**Figure 7.** Energy dissipation rates from Thorpe analysis of the radiosonde (left) and spectral analysis of the high-resolved wind measurement (right) for the BEXUS 12 flight. The cyan curve shows  $\epsilon$  in the full resolution, the blue one averages over the unstable layers detected by the Thorpe analysis ( $\langle \epsilon \rangle$ ).

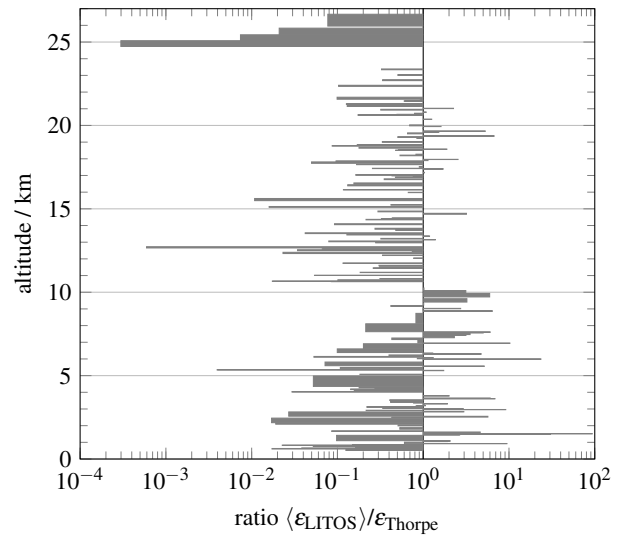


**Figure 8.** Ratio between energy dissipation rates from spectral analysis and from Thorpe analysis for the significant unstable layers of the BEXUS 12 flight.